may mix in a larger wavelength, for which the Coulomb force has a longer range.

[11]A similar calculation shows that the electron gas on the mercury chains could have a charge-density-wave transition with wave-vector components $(2k_F, 2k_F)$ in the $\vec{a}_T, \vec{b}_T$ plane.

[12]R. F. Dashen, B. Hasslacher, and A. Neveu, Phys. Rev. D 11, 3424 (1975); A. Luther, Phys. Rev. B 14, 2153 (1976).

[13]S. F. Edwards and A. Lenard, J. Math. Phys. (N.Y.) 3, 778 (1962); N. Gupta and B. Sutherland, Phys. Rev. A 14, 790 (1976).

Lithium Ordering in Li_xTiS_2

A. H. Thompson

Corporate Research Laboratory, Exxon Research and Engineering Company, Linden, New Jersey 07036

(Received 23 December 1977)

A new electrochemical measurement applied to the Li/TiS_2 cell reveals subtle changes in slope on the voltage-composition relationship. These anomalies occur at compositions where ordered structures among intercalated lithium are predicted from lattice-gas theories. Li_xTiS_2 appears to be a nearly ideal model for the study of composition- and temperature-dependent properties of the two-dimensional lattice gas.

The intercalation compounds of the layered chalcogenides with the alkali metals have received attention because of their use as battery cathodes.[1,2] In some alkali-metal intercalation compounds, such as Na in TiS_2,[3] phase boundaries occur that impede reversible intercalation, while in post-transition-metal intercalation compounds, such as Cu in NbS_2,[4] the intercalated ions are found to form ordered arrays. Such ordered structures are also found in metal-rich layered compounds such as $Ti_{1+x}S_2$[5] and $V_{1+x}Se_2$.[6] In $Ti_{1+x}S_2$ the metal ions in intercalated sites are presumably immobile at room temperature while in Na_xTiS_2 the symmetry of the site occupied by the intercalate is a function of composition.[3] In contrast to these cases the intercalated Li ions in Li_xTiS_2 are mobile at room temperature[7] and no distinct phase boundaries have been apparent for $0 < x < 1$.[7,2]

The work reported here shows that, even though Li in Li_xTiS_2 is mobile, there are subtle irregularities on the curve of intercalation energy versus composition at compositions where lattice-gas theories predict that ordered structures should occur. Six of the compositions where ordering occurs are used to conclude that the Li^+-Li^+ interaction is dominated by the long-range Coulomb repulsion. Composition- and temperature-dependent studies suggest that Li_xTiS_2 offers a uniquely versatile lattice-gas-model system on which studies may encompass the entire lattice-gas phase diagram for the Li^+-Li^+ interaction. The measurements reported here mark the first detection of such ordered structures in an electrochemical measurement.

Battery cycling data were collected using a new electrochemical technique. Quasiconstant-potential, open-circuit measurements were made by a series of constant potential steps. The potential remains fixed on each step while the current decays in time to some small value, I_{min}. When I_{min} is reached, the voltage is advanced to the next level. One complete cycle is made and the net charge, ΔQ, accumulated on each step is obtained by averaging the values on the charge and discharge portions of a cycle. This technique yields a high-resolution approximation to the open-circuit discharge curve and provides an accurate derivative of the voltage-charge relationship.

The data obtained on Li-Li_xTiS_2 are shown in Fig. 1. Figure 1(a) shows the integrated discharge curve at 300 K, while the incremental capacity at 300 K is shown in Fig. 1(b). The incremental capacity is the charge accumulated on each voltage step divided by the size of the voltage step. The raw data are actually collected in the derivative format as in (b) where the typical reproducibility is 1% of the $\Delta x/\Delta V$ values. The accumulated charge is normalized to the capacity of the cell and the voltage step is 0.01 V for all the reported data. A typical cathode has a capacity of 50 C on an area of 2 cm^2. Maximum discharge-current densities are limited to 2 mA/cm^2 and the I_{min} is 1 $\mu A/cm^2$. The cells were prepared as described previously.[2] Two cells were

© 1978 The American Physical Society

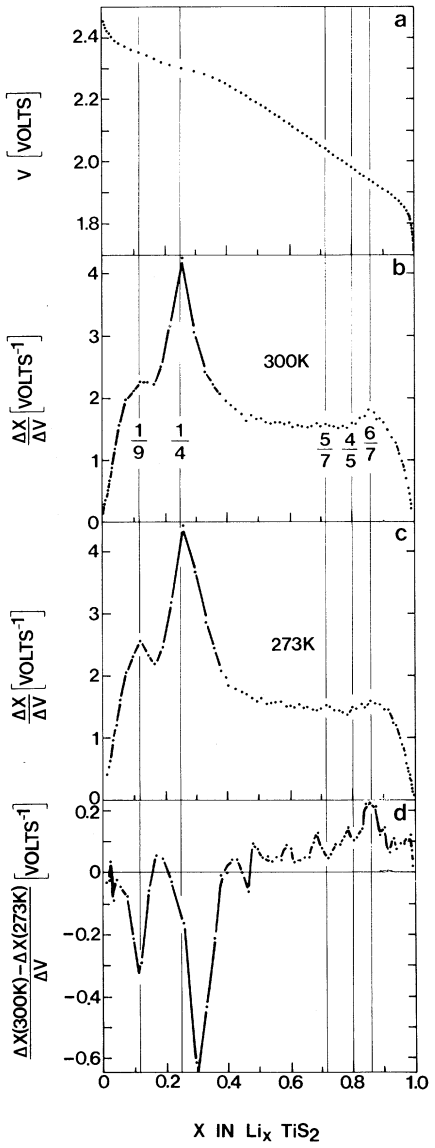

FIG. 1. (a) The quasi-open-circuit, voltage-composition relation for Li-Li_xTiS_2. (b), (c) The reciprocal derivative of (a) at 300 and 273 K. The ordinate is the incremental capacity or the charge accumulated at each datum point of (a) normalized to the total cell capacity. (d) The difference between (b) and (c) [(b) − (c)].

measured; one using high-surface-area (3 m^2/g) TiS_2 made from sponge titanium and sulfur; the other one using highly crystalline, high-purity material made from titanium wire. No differences between these cathodes were detected in these measurements. Cells containing no TiS_2 were cycled to identify spurious capacities associated with impurities, electrolyte decomposition, cathode grid reactions, etc. All such spurious capacities were found to contribute less than 0.1% to the measured capacity. The room temperature and cell temperature were measured during cell operation and no systematic errors with temperature variations were detectable.

Figure 1(b) shows peaks in incremental capacity at compositions near $X = \frac{1}{9}$, $\frac{1}{4}$, and $\frac{6}{7}$, while at 273 K, Fig. 1(c), the peak at $X = \frac{1}{9}$ is sharpened considerably, the $\frac{1}{4}$ peak is broadened to the right, and the $\frac{6}{7}$ peak is partially flattened. Figures 1(b) and 1(c) do not reveal the full resolution of the measurement and so their difference was taken as shown in Fig. 1(d). On five discharges at 273 K and two at 300 K the scatter in the data was less than 1% or approximately 0.01 V^{-1}. The reproducible features from these several cycles are indicated by the faired curve of Fig. 1(d). The data of Fig. 1(d) are averaged data from several complete cycles but those features designated reproducible appear as relative maxima on *every* data set. The data of Fig. 1(d) emphasize the sharpening of the peak at $x = \frac{1}{9}$ and show that the broadening of the $\frac{1}{4}$ peak appears as a new peak near $x = \frac{3}{10}$. In addition to the major peaks at $\frac{1}{9}$, $\frac{1}{4}$, $\frac{3}{10}$, and $\frac{6}{7}$, reproducible maxima were *always* observed at $\frac{5}{7}$ and $\frac{4}{5}$. The uncertainty in these peak positions is estimated to be ±0.01 mole and is limited by the instrumental resolution of 0.01 V. The remaining reproducible features of Fig. 1(d) are either too broad to be definitive about their placement or require higher voltage resolution to be confident of their existence. These features are the subject of continuing studies with equipment having higher resolution. Although complete cycles were always made in these experiments, the corrections introduced by cell *IR* drops, electrode polarization, and irreversible reactions were insignificant at the effective current densities of 1 $\mu A/cm^2$. The hysteresis between charge and discharge cycles is typically of the order of the instrumental resolution of 0.01 V.

I will now argue that the characteristic compositions are associated with the formation of an ordered lithium superlattice between the TiS_2 layers, and that these structures are those expected when the Li^+-Li^+ interaction is the long-range, repulsive, Coulomb interaction and the Li^+ ions are constrained to reside on a two-dimensional triangular lattice. At room temperature the Li^+ ions are mobile[7] but are constrained to reside in the octahedral, interlayer sites supplied by the TiS_2 host.[8] These octahedral sites lie on the triangular TiS_2 lattice. When there are

interactions between the Li^+ ions, such as a Coulomb or dipolar repulsion, the mobile lithium may be further constrained to occupy certain octahedral sites preferentially, thus forming a superlattice parallel to the TiS_2 planes. One such set of superlattices occurs when all near-neighbor lithiums are equidistant. On a two-dimensional, triangular-lattice equidistant structures can appear when $x = 1, \frac{1}{3}, \frac{1}{4}, \frac{1}{7}, \frac{1}{9}, \frac{1}{12}, \frac{1}{13}, \frac{1}{16}, \frac{1}{19}, \frac{1}{21}, \ldots$. As discussed by Kaburagi and Kanamori[9,10] and Kaburagi,[11] the ordered structures one expects to see on any given lattice will depend in detail on the interparticle interactions. The near-neighbor–equidistant structures are exclusively predicted for the cases where interactions to second neighbor are present.[10] When longer-range interactions are present, numerous structures are possible including structures where an ion's near neighbors are not equidistant.[11] It is the appearance of nonequidistant ordered compositions that plays a cruicial role in deciding the nature of the ion-ion interactions.

In the present electrochemical data the features at $\frac{1}{9}$ and $\frac{1}{4}$ are equidistant compositions while the $\frac{6}{7}$ composition is one where the vacant octahedral sites may form a near-neighbor–equidistant structure. The well-established features at nonequidistant compositions are those associated with vacancy ordering at $\frac{5}{7}$ and $\frac{4}{5}$. By use of the appearance of these compositions the lattice-gas model[11] may then be used to suggest the possible types of ion-ion interactions that can produce these structures. When this is done, it is found that a contiguous region of the lattice-gas phase diagram is defined that contains the repulsive Coulomb interaction but does not contain the dipolar or higher multipolar repulsions. (A dipolar or quadrupolar interaction might be expected from the positive charge on the Li and the negative charge on the TiS_2 layers.) In addition, the appearance of an ordered structure at $\frac{1}{9}$ requires the Li^+-Li^+ interaction to be long range, substantially longer than the third neighbor.

Further information regarding the Li^+-Li^+ interaction may be obtained from the additional features of Fig. 1(d). The peak at $\frac{3}{10}$ may be the expected, equidistant structure at $\frac{1}{3}$ that is shifted slightly by the temperature-dependent $\frac{1}{4}$ feature or it may be associated with the temperature dependence of both the peak position and amplitude for the $\frac{1}{4}$ peak. It may also be an additional peak centered at $\frac{3}{10}$. According to Ref. 11, a $\frac{3}{10}$ structure is expected when the Li^+-Li^+ interaction is slightly longer than the Coulomb repulsion. This last possibility is not judged likely but higher-resolution data may resolve these alternatives and clearly delineate the remaining subtlties. From this comparison of the electrochemical data and lattice gas models I conclude that all of the observed anomalies (including the more subtle features not discussed) occur at compositions where ordered structures are predicted for the repulsive Coulomb interaction between Li^+ ions.

The structural origin of the electrochemical features reported here is supported by independent x-ray studies made prior to this investigation.[12] These x-ray studies discovered irregular changes in the lattice parameters of Li_xTiS_2 in a Li-Li_xTiS_2 cell discharged in an x-ray diffractometer. Direct observation of an ordered lithium lattice is difficult because of the relatively small x-ray scattering cross section of Li compared to Ti and S, but indirect observation of such ordering may be observed in the lattice parameters and the titanium-atom positions.

The electrochemical parameters can be directly related to the thermodynamics of lithium intercalation and superstructure formation and hence supply complementary data to those obtained by structural studies. The cell potential is related to the partial molar free energy of formation of Li_xTiS_2 by $\Delta G = -nFV$ where ΔG is the free energy of formation, n is the number of electrons (= 1), and F is the Faraday. The thermodynamics of the Li-TiS_2 couple are discussed by Whittingham.[13] Additional thermodynamic information can be obtained from the incremental capacity. The thermodynamics of a reversible electrochemical cell may be described by analogy to the thermodynamics of fluids.[14] In this analogy, pressure is replaced by $-V$, the cell potential at open circuit, and volume by Q, the electric charge. The electrochemical analogy of the isothermal compressibility is then

$$k_T(\text{electrochemical}) = -\frac{1}{Q}\frac{\partial Q}{\partial V} = -\frac{1}{x}\frac{\partial x}{\partial V}.$$

The incremental capacity is then a response function for the electrochemical cell analogous to the isothermal compressibility times the charge. The peaks in $\Delta x/\Delta V$ would then be the expected response when the electrochemical system passes near a critical point, where the isothermal compressibility has a λ-point singularity. This analogy, the electrochemical data and the published diffusion studies[7] lead me to suggest that, at room temperature, Li_xTiS_2 lies near, but probably above, the critical points for ordering of the

Li^+ ions. When the composition is changed the system passes through regions of composition where ordering fluctuations occur, leading to peaks in the "compressibility." Between the compressibility peaks the lithium form a disordered liquid. With this analogy to the thermodynamics of liquid-gas systems, it is anticipated that high-resolution and temperature-dependent electrochemical studies can be used to study the Li_xTiS_2 phase diagram in detail, including critical-exponent studies near ordered compositions.

The author thanks R. R. Chianelli, J. P. de Neufville, L. B. Ebert, A. J. Jacobson, S. C. Mraw, F. A. Putnam, B. M. Rao, B. G. Silbernagel, and M. S. Whittingham for discussions. He thanks J. R. Schrieffer for helpful suggestions and J. Kanamori and M. Kaburagi for communication of unpublished work.

[1]A. H. Thompson and M. S. Whittingham, Mater. Res. Bull. 12, 741 (1977).
[2]M. S. Whittingham, Science 192, 1126 (1976), and Solid State Chem. 13, 1 (1977).
[3]B. G. Silbernagel and M. S. Whittingham, Mater. Res. Bull. 11, 29 (1976); also A. Leblanc-Soreau, M. Danot, L. Trichet, and J. Rouxel, Mater. Res. Bull. 9, 191 (1974).
[4]F. W. Boswell, A. Prodan, and J. M. Corbett, Phys. Status Solidi (a) 35, 591 (1976).
[5]A. H. Thompson, F. R. Gamble, and C. R. Symon, Mater. Res. Bull. 10, 915 (1975); J. J. Legendre, M. Huber, and M. Sauvage, Phys. Status Solidi 40, K101 (1977).
[6]E. Rost and L. Giertsen, Z. Anorg. Allg. Chem. 328, 299 (1964).
[7]B. G. Silbernagel and M. S. Whittingham, J. Chem. Phys. 64, 3670 (1976).
[8]A. J. Jacobson *et al.*, to be published.
[9]M. Kaburagi and J. Kanamori, Prog. Theor. Phys. 54, 30 (1975).
[10]M. Kaburagi and J. Kanamori, Jpn. J. Appl. Phys., Suppl. 2, 145 (1974).
[11]M. Kaburagi, Thesis, Department of Physics, Osaka University, Osaka, Japan, 1975 (unpublished).
[12]R. R. Chianelli, B. M. L. Rao, and J. Scanlon, to be published.
[13]M. S. Whittingham, J. Electrochem. Soc. 123, 315 (1976).
[14]For example, see M. W. Zemansky, *Heat and Thermodynamics* (McGraw-Hill, New York, 1957), p. 292; or a text on chemical thermodynamics such as K. Denbigh, *The Principle of Chemical Equilibrium* (Cambridge Univ. Press, Cambridge, 1971).

Experimental Band Structure and Temperature-Dependent Magnetic Exchange Splitting of Nickel Using Angle-Resolved Photoemission

D. E. Eastman, F. J. Himpsel, and J. A. Knapp
IBM Thomas J. Watson Research Center, Yorktown Heights, New York 10598
(Received 27 March 1978)

Using angle-resolved photoemission and synchrotron radiation, we have determined the energy-versus-momentum valence-band dispersion relations for a Ni(111) crystal. The temperature-dependent ferromagnetic exchange splitting has been directly observed. Both the d-band width (~3.4 eV at L) and exchange splitting (0.31 eV) are much smaller than theoretical estimates (~4.5 eV wide at L with ~0.7-eV splitting, respectively, at 293 K).

Nickel has been a prototype metal for innumerable studies of various physical properties involving itinerant-electron ferromagnetism, d-band electronic structure, and transition-metal surfaces. Despite intense study, two basic aspects of Ni have remained controversial and unresolved, i.e., the overall d-band width and the exchange splitting. For example, angle-integrated photoemission estimates of the d-band resonance width[1,2] (~3.3 eV) are narrower than self-consistent one-electron band theory estimates[3-5] (~4.5 eV). One explanation given for the observed narrow d bands is that photoemission samples only a few atomic layers and band narrowing occurs at the surface.[6,7] Another recent explanation of the narrow experimental widths is that the lower d states in Ni have very short electron hole lifetimes.[8] However, several recent angle-resolved photoemission experiments report larger widths (e.g., $\simeq$ 4.2 eV)[9] or "agree" with theory.[10,11] Photoemission, optical, and theoretical studies of the magnetic exchange split-

© 1978 The American Physical Society